

Multiphysics Simulation of Thermoelectric Systems - Modeling of Peltier-Cooling and Thermoelectric Generation

Martin Jaegle
 Fraunhofer-IPM, Heidenhofstr. 8, 79110 Freiburg, Germany
 Martin.Jaegle@ipm.fraunhofer.de
 Tel: +49 761 8857 345, Fax: +49 761 8857 224

Abstract: Electro-thermal interaction is commonly considered only as a matter of joule heating. In addition, the Seebeck-, Peltier- and Thompson-Effects are significant in materials with high thermoelectric figure of merit Z . These thermoelectric materials have a high Seebeck-coefficient α , a good electric conductivity σ , and a poor thermal conductivity λ . They have widespread areas of application. Thermoelectric systems are used for measurement techniques (thermocouples, thermopiles...), for peltier-cooling (Peltier-elements for CPU-Cooling, refrigeration, temperature stabilization...) and direct energy conversion of heat (thermoelectric generators, driven by waste heat, radioactive decay, combustion...). For an accurate modeling of these applications the thermoelectric field equations have to be solved.

Keywords: Thermoelectric Generation, Cooling, Peltier-Effect, Seebeck-Effect

1. Introduction

In this presentation an implementation of thermoelectric effects in COMSOL Multiphysics is described using the PDE-Application Mode. Therefore the coupled heat equation and Poisson's equation are extended by the thermoelectric effects and solved simultaneously, to get the solution for the field variables temperature T and voltage V :

$$-\nabla \cdot ((\sigma \alpha^2 T + \lambda) \nabla T) - \nabla \cdot (\sigma \alpha T \nabla V) = \sigma ((\nabla V)^2 + \alpha \nabla T \nabla V) \quad (1)$$

and

$$\nabla \cdot (\sigma \alpha \nabla T) + \nabla \cdot (\sigma \nabla V) = 0, \quad (2)$$

where the material properties α , σ and λ denote the thermopower (Seebeck-coefficient), the electric and the thermal conductivity, respectively. Usually those material properties depend on the temperature and may be anisotropic. Here only isotropic material properties are used at constant material parameters. The above equations can be derived from the coupled equations in [2] or the literature cited therein [3].

The FEA-Model

COMSOL- Multiphysics allows the implementation of common arbitrary partial differential equations (PDEs) of the field variable u on a one to three dimensional region Ω . Two PDE modes can be used: The "Coefficient-Form" and the "General Form". In the more didactical "Coefficient Form" PDE application mode, the program allows the definition of the coefficients for the following PDE:

$$\begin{aligned} c_n \frac{\partial^2 u}{\partial x_n^2} + d_n \frac{\partial u}{\partial x_n} + \nabla \cdot (-c \nabla u - cu + \gamma) + \beta \cdot \nabla u + cu = f & \quad \text{in } \Omega \\ n \cdot (-c \nabla u - cu + \gamma) + qu = g - h^T \mu & \quad \text{on } \partial \Omega \\ hu = r & \quad \text{on } \partial \Omega \end{aligned} \quad (3)$$

Equation (3) follows the notation of the COMSOL-Multiphysics documentation. Please notice that some symbols from the equations (1) - (2) occur also here, but with a different meaning. The first line describes the PDE, the second and third lines define the coefficients for the generalized Neumann boundary condition and the Dirichlet boundary condition on the surface of the region Ω .

The thermoelectric field equations (1) - (2) can now be transformed into the "coefficient form" as follows.

With the vector valued field variable

$$\vec{u} = \begin{pmatrix} T \\ V \end{pmatrix}, \quad (4)$$

the coefficient c in (3) is

$$c = \begin{pmatrix} \lambda + \sigma \alpha^2 T & \sigma \alpha T \\ \sigma \alpha & \sigma \end{pmatrix} \quad (5)$$

and f is

$$f = \begin{pmatrix} \sigma ((\nabla V)^2 + \alpha \nabla T \nabla V) \\ 0 \end{pmatrix} \quad (6)$$

The other coefficients in equation (3) are zero for static calculations.

For transient calculations, capacitive influences have to be respected. Mostly it is sufficient to consider only the thermal capacity (heat capacity C , density ρ). Then d in equation (3) is

$$d = \begin{pmatrix} \rho C \\ 0 \end{pmatrix} \quad (7)$$

For the implementation of the PDE coefficients into COMSOL the notation for deviations is

$$\frac{\partial V}{\partial x} = V_x, \quad \frac{\partial V}{\partial t} = V_t, \quad \frac{\partial^2 V}{\partial x \partial t} = V_{tx}, \quad \vec{\nabla} V = (V_x \quad V_y \quad V_z) \quad (9)$$

Examples

The following examples show results of calculations for typical thermoelectric applications. The material properties for the calculations with temperature independent values are shown in table 1. Here typical values for Bismuth-Telluride and copper were taken from [2]. Temperature dependent material properties were taken manually from figure 7 in [4]. They were interpolated by cubic splines (figure 1-3). For the copper electrodes no temperature dependency was used.

Table 1: Numerical material properties from [2]

		Thermoelectric Material	Electrode (Copper)
Seebeck Coefficient	α , V/K	p: 200e-6 n: -200e-6	6.5e-6
Electric conductivity	σ , S/m	1.1e5	5.9e8
Thermal conductivity	λ , W/m/K	1.6	350
Density	ρ , kg/m ³	7740	8920
Heat capacity	C, J/kg/K	154.4	385

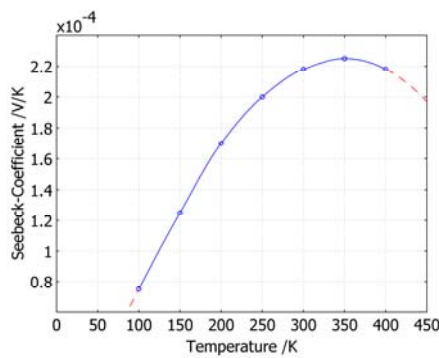


Figure 1: Temperature dependent Seebeck coefficient of $(\text{Bi}_{0.5}\text{Sb}_{0.5})_2\text{Te}_3$ taken from [4] and cubic spline interpolation.

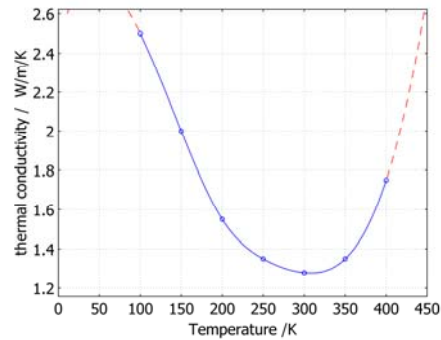


Figure 2: Temperature dependent thermal conductivity of $(\text{Bi}_{0.5}\text{Sb}_{0.5})_2\text{Te}_3$ [4].

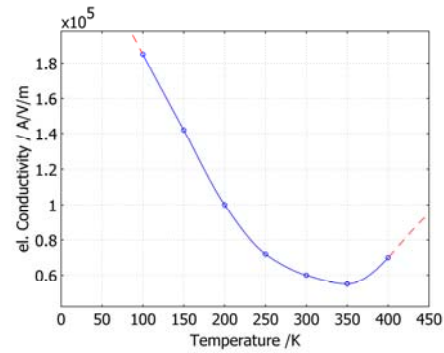


Figure 3: Temperature dependent electric conductivity of $(\text{Bi}_{0.5}\text{Sb}_{0.5})_2\text{Te}_3$ [4].

Table 2: Temperature dependent material properties of $(\text{Bi}_{0.5}\text{Sb}_{0.5})_2\text{Te}_3$ from [4].

T /K	α / 10^6 V/K	λ / W/m/K	σ / 10^3 A/V/m
100	75	2.5	185
150	125	2	142
200	170	1.55	100
250	200	1.35	72
300	218	1.28	60
350	225	1.35	55
400	218	1.75	70

Example 1: Thermoelectric Cooler

A simple cooler geometry consists of one p-type semiconductor element $1 \times 1 \times 5.8 \text{ mm}^3$ in size. It is contacted by two copper electrodes 0.1 mm in thickness (Figure 4).

Table 1 shows the material properties used for temperature-independent calculations. The boundary conditions were set to 0V and 0°C at the base of the lower electrode. Adiabatic boundary conditions were taken on all other surfaces. At the top of the upper electrode a current of 0.7A was applied.

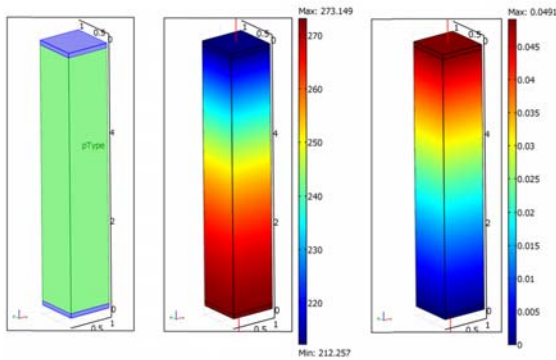


Figure 4: A p-type thermoelectric element is contacted by copper electrodes (left). The base is kept at 0°C and 0V. At the top 0.7A current was applied. Adiabatic boundary conditions were used. The resulting temperature distribution is shown in the center, the voltage is shown right. A temperature difference of nearly 61 K is achieved. The voltage at the upper electrode is 49 mV.

Figure 4 shows the result of the calculation. In the center, the temperature distribution shows that the cold side temperature is at 212.26K. The associated voltage is shown right. To drive the current, a voltage of 49.1mV is needed.

The same calculations were made with temperature dependent material properties. Figure 5 shows the cold side temperatures for temperature dependent (crossed curve) and constant material properties (circles). In addition, a heat load of 10mW was applied at the cold side. The elements have their maximum temperature difference at different currents according to the different material properties.

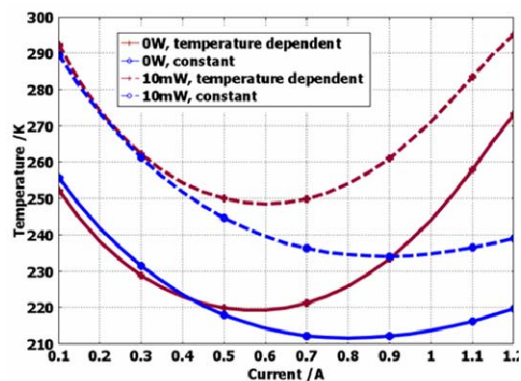


Figure 5: Calculated cold side temperatures versus current for constant (circle) and temperature dependent material properties (cross) without (solid) and with 10mW heat load (dotted), respectively.

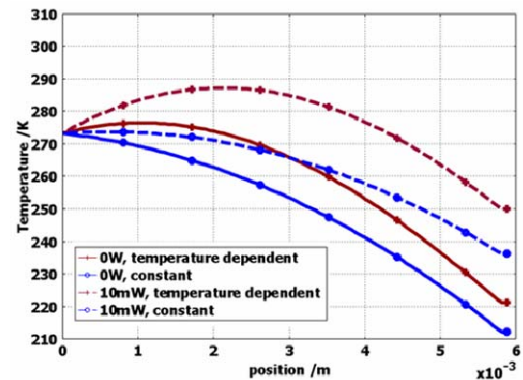


Figure 6: Temperature distribution along the element calculated with constant (circle) and temperature dependent material properties (cross) without (solid) and with 10mW heat load (dotted) on top of the element, respectively.

The temperature and voltage distribution along the element is shown in Figure 6 and 7 for a current of 0.7A.

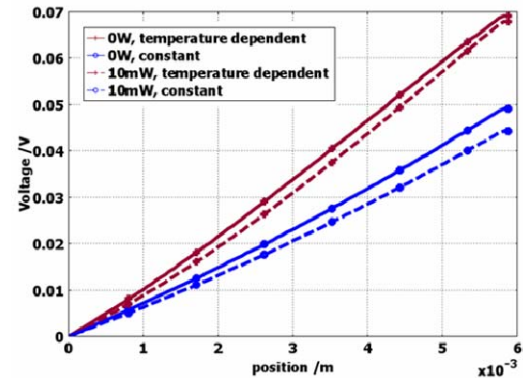


Figure 7: Voltage distribution along the element calculated with constant (circle) and temperature dependent material properties (cross) without (solid) and with 10mW heat load (dotted) on top of the element, respectively.

Example 2: Transient Operation

Figure 8 shows the result of a time dependent calculation. The above thermoelectric element is operated at 0.6 Ampere with no heat load at steady state temperatures. One second after the beginning of the calculation, the current is increased to 0.8A linearly within 0.1s. After 4 seconds the amperage decreases again linearly within 0.1s to 0.6A (figure 8, upper diagram). The lower diagram shows the transient cold side temperature with temperature dependent material parameters. The short current pulse causes a temporary temperature drop of about 3K. Such supercooling effects are also described

e.g. numerically in [2] and, in addition, experimentally in [5].

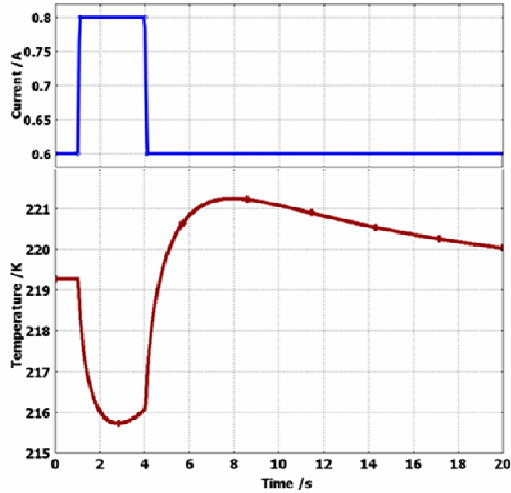


Figure 8: Transient calculation of peltier-supercooling. A short current pulse generates temporarily lower cold side temperatures.

Example 3: Thermoelectric generation

To simulate a thermoelectric generator, also the above shown semiconductor element was used, again with the variable material properties (figure 1 – 3). The top of the upper electrode was set to 100°C, the base of the lower electrode to 0°C, 0V. Figure 9: shows as a result the current-voltage and the current power characteristics of the generator.

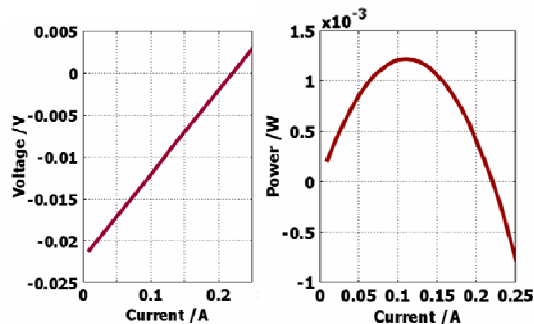


Figure 9: Current-voltage (left) and current-power characteristics (right) for the upper thermoelectric element

According to these characteristics, the open circuit voltage of the element is calculated to be about -21mV, the short-circuit current is about 220mA. The maximum power output is 1.22mW.

Example 4: Arbitrary Geometries

Many real life applications have more complex geometries, like thermopile sensors or thin film devices. One typical example where FEA is advantageous is an electrode configuration which is in the direction of the temperature gradient. Thus, the often better thermal and electrical conductance of the electrodes will shorten both, the temperature differences as well as generated voltages. Figure 10 shows such a configuration. The size of the thermoelectric material is 1x5x0.8mm³, the electrode size is 1x3x0.1mm³. The temperature on top of the configuration is set to 10°C, the base is set to 0°C. The left figure shows the temperature distribution, the figure in the middle shows the voltage. The open circuit voltage at the upper left electrode is calculated to be -2.02mV. Both shortings of the field variables by the electrodes can be seen clearly, since the steepest gradient is between the electrodes. Figure 10 shows on the right side the electric current streamlines.

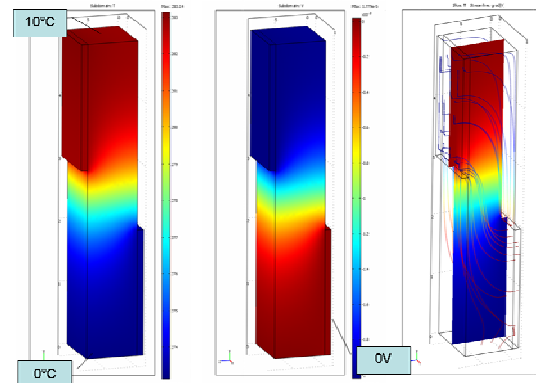


Figure 10: Example for a more “complex” element geometry: The copper electrodes are laterally connected (with respect to the temperature gradient). Left side: Temperature distribution, the top is set to 10°C, the base is at 0°C. The appropriate Voltage is shown in the middle; the left graph shows the voltage color coded electric streamlines and the temperature as a slice plot.

Example 5: Combination of thermoelectric and structural mechanic modeling

This example shows results of calculations for a p-n thermocouple, contacted by copper electrodes on a alumina substrate (Figure 11). The dimensions of the thermoelectric legs are 1.5x1.5x10mm³ with 0.5mm spacing. The electrodes are made from 0.2mm copper, the thickness of the alumina substrate is 0.5mm. The left side is kept at 0°C and is mechanically fixed. The current density J is applied at the upper left electrode, the lower left electrode is grounded.

For reasons of simplicity, neither temperature dependency of the material data, nor transient or unisotropic calculations were taken into account. The thermoelectric material data are shown in table 1. The thermal conductivity of the alumina substrate was set to 29W/m/K.

The elastic moduli and thermal expansion coefficients for bismuth-telluride are taken from [6] and are listed in table 3. The mechanic properties for copper and alumina are taken from the COMSOL material library., Young's modulus was 110GPa for copper and 300 GPa for alumina, Poissons ratio was 0.35 for copper and 0.22 for alumina. The temperature expansion coefficient was $17 \cdot 10^{-6}/K$ for copper and $8 \cdot 10^{-6}/K$ for alumina. Reference Temperature for the thermal expansion was $0^{\circ}C$.

Table 3: elastic material properties c_{ij} in $10^{11}dyn/cm^2$ at 280K and temperature expansion coefficient a_i in $10^{-6}/K$ of Bi_2Te_3 at 300K, from [4]

c_{11}	c_{66}	c_{33}	c_{44}	c_{13}	c_{14}
6.847	2.335	4.768	2.738	2.704	1.325

a_x	a_y	a_z
21.3	14.4	14.4

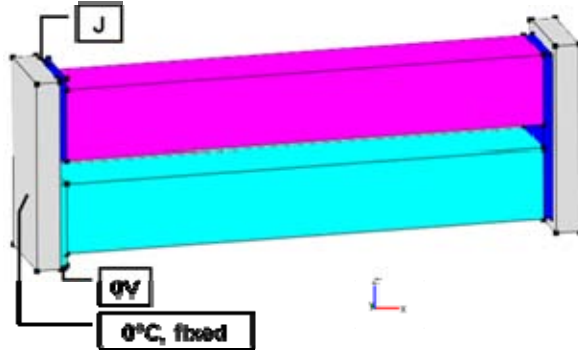


Figure 11: The thermocouple example consists of two $1.5 \times 1.5 \times 10mm^3$ legs. They are contacted with copper on a alumina substrate. The left side is kept at $0^{\circ}C$ and mechanically fixed. The current density J is applied at the upper left electrode, the lower electrode is grounded.

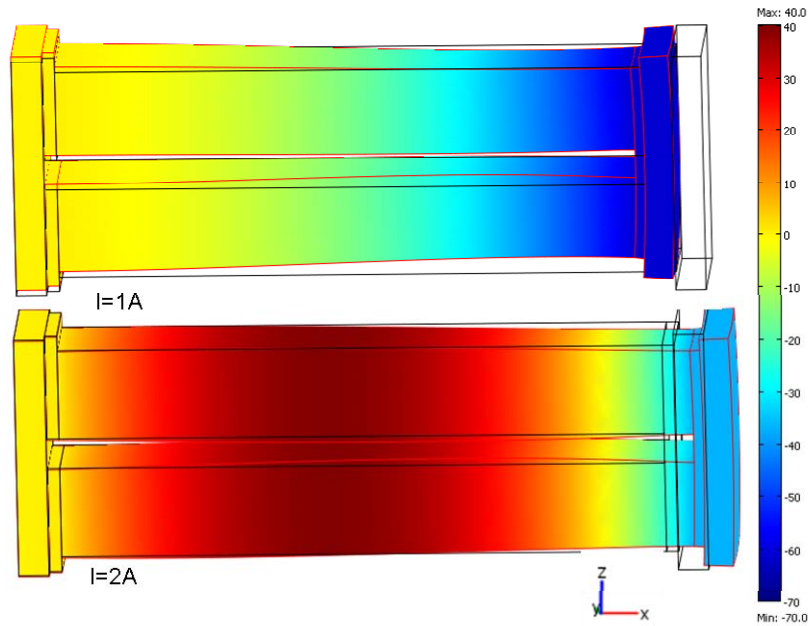


Figure 12: The thermal expansion of the thermocouple for 1A and 2A current. The initial geometry is shown as a black wireframe; the deformed frame is red and filled with temperature coded colors ($^{\circ}C$). At maximum cooling near 1A, the module shrinks about 5 microns (above). At 2A, the module is thermally expanded although it is still cooling.

To solve the PDEs, the "parametric segregated solver" in COMSOL was used. The current was varied from 0.001 - 2A. Figure 12 shows the result

for two currents, 1A above and 2A below. The original geometry is shown as a black wireframe, the displacement by thermal expansion is indicated

by the red wireframe, filled with temperature coded color.

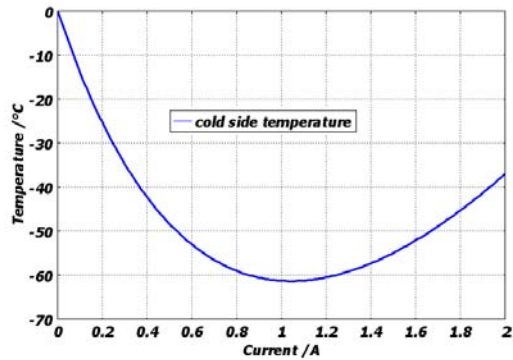


Figure 13: The calculated cold side temperature versus current shows a maximum temperature difference of about 62°C.

At maximum cooling near 1A, the module shrinks about 5 microns (above). At 2A, the module is thermally expanded although it is still cooling.

Figure 13 shows the calculated cold side temperature versus the applied current for an operation as a peltier module. About 62°C temperature difference can be achieved at 1 A.

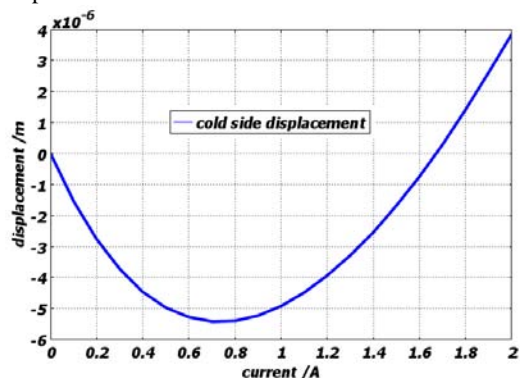


Figure 14: thermal expansion of the module in x-direction

The according change of the module length in x-direction is shown in Figure 14. At low currents, the module shrinks due to the cooling. With higher temperatures the module expands. Minimum size and maximum cooling are not at the same current.

With this model, thermoelectric and thermomechanic effects can be simulated simultaneously, and thus enabling thermomechanic studies of thermoelectric effects. As an example the effect of a changed electric resistivity is shown in the figures 15 and 16. The electric resistivity of the lower thermoelectric leg was doubled.

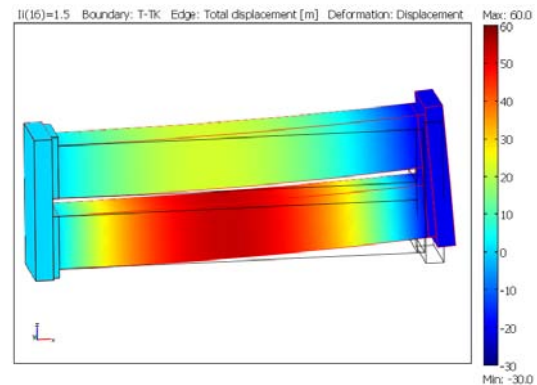


Figure 15: A doubling of the resistivity of the lower thermoelectric leg leads to higher temperatures and thus to asymmetric thermal expansion. Other parameters are like in figure 2, the current is 1.5A.

Figure 5 shows the calculated temperature distribution and thermal expansion for a current of 1.5A. The different resistivities of the thermoelectric legs lead to an asymmetric temperature distribution in the legs, causing a bending of them due to the thermal expansion. Figure 6 shows the von Mises stress within the module as a slice Plot. A maximum stress of about 37MPa was calculated.

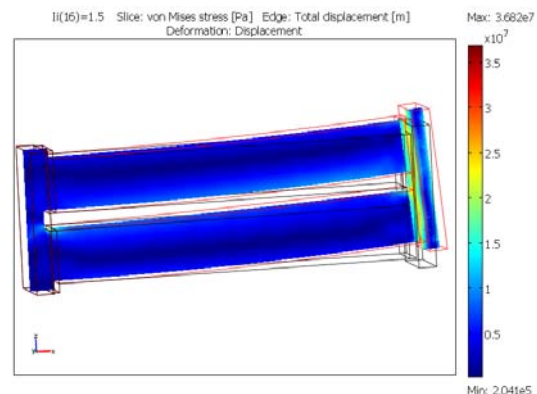


Figure 16: Von Mises stress in the asymmetrically strained module of figure 15.

Summary

An implementation of the thermoelectric field equations in COMSOL multiphysics is shown. Thermoelectric calculations can be made for arbitrary geometries. Anisotropy (not shown) and temperature dependency of the materials can be included. Also transient calculations can be made. Structural analysis or convection can also be added easily.

Parts of this Publication were published previously in [7] - [9].

Literature

- [1]: COMSOL Multiphysics 3.3a Documentation, www.comsol.com
- [2]: Antonova E.E., Looman D.C; Finite Elements for Thermoelectric Device Analysis in ANSYS; Int. Conference on Thermoelectrics; 2005 pp. 200
- [3]: Landau, L. D. and Lifshitz, E. M.; Electrodynamics of Continuous Media, 2nd Edition, Butterworth Heinemann (Oxford, 1984)
- [4]: Seifert, W., Ueltzen, M., Müller, E.; One Dimensional Modelling of Thermoelectric Cooling; phys.stat.sol. (a) 194, No.1, pp 277 – 290; 2002
- [5]: Snyder, G.J. et al; Supercooling of Peltier cooler using a current pulse; J. Appl. Phys; Vol. 92, No. 3; pp. 1564-1569, 2002
- [6]: Landolt-Börnstein; Numerical data; ISBN3540121609; Vol 17f, pp.275, 1983
- [7]: 1. Jaegle, Martin; Simulating Thermo-electric Effects with Finite Element Analysis using COMSOL; Proceedings ECT2007, Odessa; p.222
- [8]: Martin Jaegle, Markus Bartel, Dirk Ebling, Alexandre Jacquot Harald Böttner; Multiphysics simulation of thermoelectric systems; Proceedings ECT2008, Paris, O27-1
- [9]: Dirk Ebling, Martin Jaegle, Markus Bartel, Alexandre Jacquot, Harald Böttner; Multiphysics simulation of thermoelectric systems for the comparison to experimental device performance; Proceedings ICT 2008, To be published